Two-photon nonlinearity by an excitonic system placed in a cavity

Kazuki Koshino[1,3,*] and Hajime Ishihara[2,3]
[1]*Faculty of Systems Engineering, Wakayama University, 930 Sakaedani, Wakayama 640-8510, Japan*
[2]*Department of Physics and Electronics, Graduate School of Engineering, Osaka Prefecture University, 1-1 Gakuen-cho, Sakai, Osaka 599-8531, Japan*
[3]*CREST, Japan Science and Technology Agency, 4-1-8 Honcho, Kawaguchi, Saitama 332-0012, Japan*
(Received 28 December 2004; published 24 June 2005)

We have investigated the two-photon nonlinearity attained by a finite-sized excitonic system placed inside of a cavity, paying attention to the dependence on the system size N. The two-photon nonlinearity is evaluated by utilizing semiclassical optical responses. In the quantum-dot limit, the excitonic system behaves as a single two-level system with an enhanced coupling to the cavity mode. In the bulk limit, the nonlinear phase shift decreases as N is increased, proportionally to $N^{-1/2}$.

DOI: 10.1103/PhysRevA.71.063818 PACS number(s): 42.50.Pq, 42.65.−k

I. INTRODUCTION

Strong nonlinear optical effects are expected by strong input fields. It is therefore natural that strong laser beams are usually used in conventional nonlinear optical spectroscopy [1]. However, by exploiting the idea that the electric field can be amplified inside of a cavity and therefore that the optical nonlinearity of a material can be effectively enhanced when it is placed inside of a cavity, it was experimentally demonstrated that significant nonlinear optical effects can be induced even by extremely weak input fields [2,3]. Encouraged by this experimental demonstration and also by the remarkable progress in photon manipulation techniques [4–6], interest in the nonlinear optical effect between two photons is rapidly growing. The possibility of applying the two-photon nonlinearity to quantum logic gates has also activated this research field [7,8].

Theoretically, the nonlinear dynamics of two photons has been investigated when the nonlinear system is a two-level system placed inside of a cavity [9,10], whose optical nonlinearity originates solely in the saturation effect of the two-level system. It was shown there that a significant nonlinear phase shift may be induced in the two-photon wave function, provided that the frequency and coherent length of input photons are optimally chosen. In order to design compact devices, it is desirable to use a solid-state nonlinear material, which, however, cannot generally be described by a two-level system due to large mechanical degrees of freedom. In the present study, we wish to evaluate the two-photon nonlinearity attained by a finite-sized nonlinear system, such as molecular aggregates and solid-state media. There are two naive expectations concerning this problem: On the one hand, the oscillator strength between ground and excited states may concentrate on a specific mode of excited states, which results in an enhancement of $\chi^{(3)}$ [11] and, therefore, of the two-photon nonlinearity. On the other hand, the saturation effect becomes weaker as the system size is enhanced, which would be disadvantageous for nonlinear effects. The interplay between these opposite effects will be clarified in the following sections.

This study is presented as follows. Section. II serves as a statement of the problem, where the quantum-mechanical Hamiltonian for the nonlinear system and photons is given, and the measure β of the two-photon nonlinearity is defined. In Sec. III, we present the evaluation method for the two-photon nonlinearity, which is based on the semiclassical optical response [12]. In Sec. IV, we actually evaluate the two-photon nonlinearity numerically, using three concrete forms of V_{ji} (the exciton hopping interaction). It is demonstrated there that qualitatively the same results are obtained regardless of the form of V_{ji}. In Sec. V based on the mean-field form of V_{ji}, the dependence on the system size is investigated, both analytically and numerically. We discuss two limiting cases—namely, the quantum-dot limit and the bulk limit—and observe the crossover between two limits. The main results are summarized in Sec. VI.

II. THEORETICAL MODEL

A. System and Hamiltonian

Our main concern in this study is to evaluate the two-photon nonlinearity attained by a finite-sized nonlinear material. As the model of such a nonlinear material, we employ a Frenkel excitonic system composed of N sites. In this model, each site works as a two-level quantum system. The model is therefore applicable not only to molecular aggregates but also to other systems, such as an assembly of quantum dots. Furthermore, it is known that the picture of a Frenkel exciton is also valid in semiconducting materials with a strong excitonic effect. This system is placed inside of a one-sided cavity, as illustrated in Fig. 1. Here, we consider a lossless limit where the nonlinear material is not coupled to noncavity modes. (In the conventional notations of cavity QED [13], $\gamma=0$.) The right-side mirror is weakly transmissive, through which the cavity mode is connected to an external photon field. The external photon field is labeled one dimensionally by r. Although the external field actually extends only in the $r>0$ region and the incoming and outgoing photons are traveling in the opposite direction, one may treat

*Electronic address: ikuzak@sys.wakayama-u.ac.jp

 ©2005 The American Physical Society

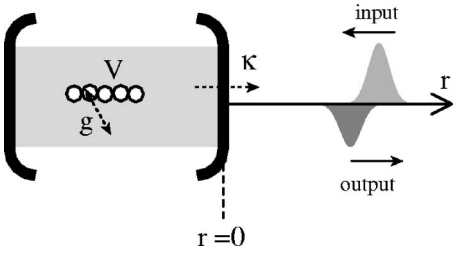

FIG. 1. Illustration of the exciton-cavity system. The cavity mode is connected through the right mirror to the external photon field. g, κ, and V represent the coupling between the cavity mode and a single site, the escape rate of a cavity-mode photon, and the hopping interaction between sites, respectively.

the incoming photons as if they were propagating in the $r<0$ region in the positive direction [14].

Hereafter, taking $\hbar=c=1$, the Hamiltonian of the whole system is given by

$$\mathcal{H}=\omega_a\sum_j s_j^\dagger s_j+\omega_c c^\dagger c+g\sum_j (s_j^\dagger c+c^\dagger s_j)+\sum_{j\neq i} V_{ji}s_j^\dagger s_i + \int dk k b_k^\dagger b_k+\int dk[(\kappa/2\pi)^{1/2}c^\dagger b_k+\text{H.c.}], \tag{1}$$

where s_j, c, and b_k are the annihilation operators for the excitation in the jth site, the cavity mode, and the external photon mode with wave number k, respectively. c and b_k are bosonic operators satisfying $[c,c^\dagger]=1$ and $[b_k,b_q^\dagger]=\delta(k-q)$, whereas s_j is the Pauli matrix satisfying $[s_j,s_i^\dagger]=\delta_{ji}(1-2s_j^\dagger s_j)$. The physical meanings of the parameters are as follows: N is the number of sites (hereafter referred to as system size), ω_a is the transition energy at each site, ω_c is the frequency of the cavity mode, g is the coupling energy between the cavity mode and each site, V_{ji} is the hopping interaction between jth and ith sites (the concrete forms of V_{ji} are given in Sec. IV), and κ is the inverse of the lifetime of the cavity mode. It is assumed that the spatial extension of the nonlinear system is much smaller than the cavity length, and g is taken to be independent of the site index j.

B. Input and output photon states

We here introduce the real-space representation of external photon field. It is given, as the Fourier transform of b_k, by

$$b_r=(2\pi)^{-1/2}\int dk e^{ikr}b_k. \tag{2}$$

As has been noted, the negative- (positive-) r region corresponds to the input (output) port.

The input photons are localized in the negative-r region. Restricting ourselves to a case where two input photons have identical wave functions, the input photon state is given by

$$|\Psi_{\text{in}}\rangle=\int dr_1 dr_2 \psi_{\text{in}}(r_1)\psi_{\text{in}}(r_2)b_{r_1}^\dagger b_{r_2}^\dagger|0\rangle, \tag{3}$$

where $\psi_{\text{in}}(r)$ is normalized as $\int dr|\psi_{\text{in}}(r)|^2=2^{-1/2}$ and $\psi_{\text{in}}(r)=0$ in $r>0$. Throughout this study, we employ the Gaussian wave packet for input photons:

$$\psi_{\text{in}}(r)=\left(\frac{1}{\pi d^2}\right)^{1/4}\exp\left[-\left(\frac{r-a}{d}\right)^2+\text{i}(q+\omega_c)(r-a)\right], \tag{4}$$

which is characterized by the coherent length d and the central frequency q (measured from ω_c). a (<0) is an irrelevant parameter denoting the initial position of the photons.

Well after the interaction with the nonlinear material inside of the cavity, both of the two input photons will appear in the output port ($r>0$). Its state vector can be written as

$$|\Psi_{\text{out}}\rangle=\int dr_1 dr_2 \psi_{\text{out}}(r_1,r_2)b_{r_1}^\dagger b_{r_2}^\dagger|0\rangle, \tag{5}$$

where $\psi_{\text{out}}(r_1,r_2)=\psi_{\text{out}}(r_2,r_1)$ and $\psi_{\text{out}}(r_1,r_2)$ is normalized as $\int dr_1 dr_2|\psi_{\text{out}}(r_1,r_2)|^2=2^{-1}$. Contrarily to the input wave function, Eq. (3), the two-photon wave function is no more separable; namely, correlation is generated between two photons in the output state.

C. Measure of two-photon nonlinearity

Here, we introduce a measure for evaluating the two-photon nonlinearity appearing in the output state. As is well known, the classical field amplitude vanishes for the photon number states [15], so conventional quantifications of nonlinear optical response cannot be employed here. To the end of evaluating the nonlinearity for the two-photon states, we compare the output wave function $|\Psi_{\text{out}}\rangle$ with the *linear* output wave function $|\Psi_{\text{out}}^{\text{L}}\rangle$, which is defined by

$$|\Psi_{\text{out}}^{\text{L}}\rangle=\int dr_1 dr_2 \psi_{\text{out}}^{\text{L}}(r_1)\psi_{\text{out}}^{\text{L}}(r_2)b_{r_1}^\dagger b_{r_2}^\dagger|0\rangle, \tag{6}$$

where $\psi_{\text{out}}^{\text{L}}(r)$ is the one-photon output wave function, which would be obtained as a resultant of a one-photon input, $\int dr\psi_{\text{in}}(r)a_r^\dagger|0\rangle$. Such a linear response would be obtained when the nonlinearity of the system is completely removed. (In the present case, each site is replaced with a harmonic oscillator with frequency ω_c.)

As the measure of nonlinearity, we employ the overlap of $|\Psi_{\text{out}}^{\text{L}}\rangle$ and $|\Psi_{\text{out}}\rangle$:

$$\beta=\langle\Psi_{\text{out}}^{\text{L}}|\Psi_{\text{out}}\rangle=2\int dr_1 dr_2 \psi_{\text{out}}^{\text{L}*}(r_1)\psi_{\text{out}}^{\text{L}*}(r_2)\psi_{\text{out}}(r_1,r_2). \tag{7}$$

$|\beta|\leqslant 1$ by definition, and $\beta\to 1$ in the limit of completely linear response. In the following part of this study, $|\beta-1|$ is often used as a real quantity representing the magnitude of nonlinearity. The complex quantity $\beta(=|\beta|e^{i\theta})$ has two physical meanings. The phase θ represents the nonlinear phase shift in the output wave function. On the other hand, the absolute value $|\beta|$ represents the difference in the shape of the linear and nonlinear output wave functions: Deviation of $|\beta|$ from unity represents the degree of deformation of the output wave function from the linear output.

III. EVALUATION METHOD OF TWO-PHOTON NONLINEARITY

A. Use of the semiclassical method

In the following part of this study, we evaluate the two-photon nonlinearity β based on the model presented in Sec. II A as a function of several parameters, such as the system size N. In order to evaluate β, in principle, the output wave functions [$\psi^{L}_{\mathrm{out}}(r)$ and $\psi_{\mathrm{out}}(r_1,r_2)$] should be determined by solving the Schrödinger equation using the Hamiltonian, Eq. (1). It is usually a heavy theoretical task to follow the quantum dynamics of the whole system, treating both the nonlinear material and the photon field quantum mechanically. However, as for evaluation of β, it has been revealed that one can evaluate β in terms of the semiclassical theory [12], in which the external photon field is treated as a c-number classical field. The calculation of optical response in the semiclassical framework is much simpler task than a fully quantum-mechanical one, which allows us to evaluate β even for complicated nonlinear systems, as is discussed here. The prescription to connect the semiclassical results with the two-photon nonlinearity β is given as follows: (i) Calculate the linear and the third-order nonlinear components of the output field [denoted by $f^{(1)}_{\mathrm{out}}(r)$ and $f^{(3)}_{\mathrm{out}}(r)$, respectively] against a classical input pulse whose shape $f_{\mathrm{in}}(r)$ is given by $f_{\mathrm{in}}(r)=\psi_{\mathrm{in}}(r)$. Therefore, $f_{\mathrm{in}}(r)$ is normalized as $\int dr|f_{\mathrm{in}}(r)|^2 = 2^{-1/2}$, which means that $2^{-1/2}$ photons are contained in this classical pulse in average. (ii) Then, the two-photon nonlinearity is evaluated by

$$\beta = 1 + 2\int dr[f^{(1)}_{\mathrm{out}}(r)]^* f^{(3)}_{\mathrm{out}}(r). \tag{8}$$

The condition under which this prescription becomes valid is that two photons appear in the output port without leaving any excitations in the system. This condition is satisfied in the present model, where the lossless limit ($\gamma=0$) is considered.

B. Equations of motion

Now we proceed to investigate the optical response against a weak classical input pulse, using the semiclassical approximation. With the help of the input-output theory [15], the Heisenberg equations of motion for c and s_m are given by

$$\frac{d}{dt}c = (-\mathrm{i}\omega_c - \kappa/2)c - \mathrm{i}g\sum_j s_j - \mathrm{i}\sqrt{\kappa}b_{t_0-t}(t_0), \tag{9}$$

$$\frac{d}{dt}s_m = -\mathrm{i}\omega_a s_m - \mathrm{i}\sum_{j(\neq m)} V_{mj}s_j - \mathrm{i}gc + 2\mathrm{i}gs^\dagger_m s_m c + 2\mathrm{i}\sum_{j(\neq m)} s^\dagger_m s_m s_j, \tag{10}$$

where the initial moment is denoted by t_0. $b_{t_0-t}(t_0)$ in Eq. (9) is the initial-moment operator $b_r(t_0)$ of the external photon field in the space representation [defined in Eq. (2)] with the space coordinate $r=t_0-t$. The output field is given, in terms of the input field and the cavity mode, by

$$b_r(t) = -b_{r-t+t_0}(t_0) + \mathrm{i}\sqrt{\kappa}c(t-r). \tag{11}$$

The semiclassical approximation is executed by replacing the field operator $b_r(t_0)$ at the initial moment with a c-number field amplitude $f_{\mathrm{in}}(r)$. Hereafter choosing the origin of frequency at ω_c and denoting $\omega_a-\omega_c=\Omega$, the above equations are rewritten in the following form:

$$\frac{d}{dt}c = -\frac{\kappa}{2}c - \mathrm{i}g\sum_j s_j - \mathrm{i}\sqrt{\kappa}f_{\mathrm{in}}(t_0-t), \tag{12}$$

$$\frac{d}{dt}s_m = -\mathrm{i}\Omega s_m - \mathrm{i}\sum_{j(\neq m)} V_{mj}s_j - \mathrm{i}gc + 2\mathrm{i}gs^\dagger_m s_m c + 2\mathrm{i}\sum_{j(\neq m)} s^\dagger_m s_m s_j, \tag{13}$$

from which equations of motion for mean values of operators are derived. We solve them perturbatively. We denote the linear and third-order components of $\langle s_m\rangle$ ($\langle c\rangle$) by $\langle s_{1,m}\rangle$ and $\langle s_{3,m}\rangle$ ($\langle c_1\rangle$ and $\langle c_3\rangle$). The first-order quantities evolve as

$$\frac{d}{dt}\langle c_1\rangle = -\frac{\kappa}{2}\langle c_1\rangle - \mathrm{i}g\sum_j \langle s_{1,j}\rangle - \mathrm{i}\sqrt{\kappa}f_{\mathrm{in}}(t_0-t), \tag{14}$$

$$\frac{d}{dt}\langle s_{1,m}\rangle = -\mathrm{i}\Omega\langle s_{1,m}\rangle - \mathrm{i}\sum_{j(\neq m)} V_{mj}\langle s_{1,j}\rangle - \mathrm{i}g\langle c_1\rangle. \tag{15}$$

The equations of motion for the second-order quantities are given by

$$\frac{d}{dt}\langle s^\dagger_m s_n\rangle = \mathrm{i}\sum_{j(\neq m)} V_{jm}\langle s^\dagger_j s_n\rangle - \mathrm{i}\sum_{j(\neq n)} V_{nj}\langle s^\dagger_m s_j\rangle - \mathrm{i}g(\langle s^\dagger_m c\rangle - \langle s^\dagger_n c\rangle^*), \tag{16}$$

$$\frac{d}{dt}\langle s^\dagger_m c\rangle = \left(\mathrm{i}\Omega - \frac{\kappa}{2}\right)\langle s^\dagger_m c\rangle + \mathrm{i}\sum_{j(\neq m)} V_{jm}\langle s^\dagger_j c\rangle - \mathrm{i}g\sum_j \langle s^\dagger_m s_j\rangle + \mathrm{i}g\langle c^\dagger c\rangle - \mathrm{i}\sqrt{\kappa}f_{\mathrm{in}}(t_0-t)\langle s_{1,m}\rangle^*, \tag{17}$$

$$\frac{d}{dt}\langle c^\dagger c\rangle = -\kappa\langle c^\dagger c\rangle + \mathrm{i}g\sum_j (\langle s^\dagger_j c\rangle - \mathrm{c.c.}) + [\mathrm{i}\sqrt{\kappa}f^*(t_0-t)\langle c_1\rangle + \mathrm{c.c.}], \tag{18}$$

$$\frac{d}{dt}\langle s_m s_n\rangle = -2\mathrm{i}\Omega\langle s_m s_n\rangle - \mathrm{i}\sum_{j(\neq m)} V_{mj}\langle s_j s_n\rangle - \mathrm{i}\sum_{j(\neq n)} V_{nj}\langle s_m s_j\rangle - \mathrm{i}g(\langle s_n c\rangle + \langle s_m c\rangle), \tag{19}$$

$$\frac{d}{dt}\langle s_m c\rangle = \left(-\mathrm{i}\Omega - \frac{\kappa}{2}\right)\langle s_m c\rangle - \mathrm{i}\sum_{j(\neq m)} V_{mj}\langle s_j c\rangle - \mathrm{i}g\langle cc\rangle - \mathrm{i}g\sum_j \langle s_m s_j\rangle - \mathrm{i}\sqrt{\kappa}f_{\mathrm{in}}(t_0-t)\langle s_{1,m}\rangle, \tag{20}$$

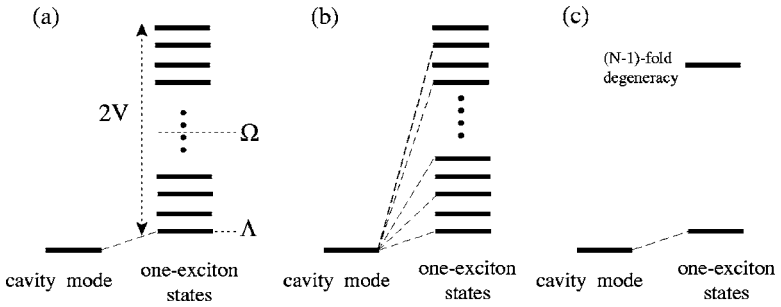

FIG. 2. The energy diagram for one-exciton eigenstates for the models (i), (ii), and (iii). The eigenenergy of the lowest one-exciton state is denoted by Λ. The higher-energy level of the one-exciton states in the model (iii) has $(N-1)$-fold degeneracy. The dashed lines connecting the cavity mode and the one-exciton states represent nonvanishing coupling.

$$\frac{d}{dt}\langle cc\rangle = -\kappa\langle cc\rangle - 2ig\sum_j \langle s_j c\rangle - 2i\sqrt{\kappa} f_{\rm in}(t_0-t)\langle c_1\rangle. \tag{21}$$

The equations of motion for the third-order quantities are given by

$$\begin{aligned}\frac{d}{dt}\langle s_m^\dagger s_n s_l\rangle =& -i\Omega\langle s_m^\dagger s_n s_l\rangle + i\sum_{j(\neq m)} V_{jm}\langle s_j^\dagger s_n s_l\rangle \\ & - i\sum_{j(\neq n)} V_{nj}\langle s_m^\dagger s_j s_l\rangle - i\sum_{j(\neq l)} V_{lj}\langle s_m^\dagger s_n s_j\rangle \\ & + ig(\langle c^\dagger s_n s_l\rangle - \langle s_m^\dagger s_l c\rangle - \langle s_m^\dagger s_n c\rangle),\end{aligned} \tag{22}$$

$$\begin{aligned}\frac{d}{dt}\langle s_m^\dagger s_n c\rangle =& -\frac{\kappa}{2}\langle s_m^\dagger s_n c\rangle + i\sum_{j(\neq m)} V_{jm}\langle s_j^\dagger s_n c\rangle - i\sum_{j(\neq n)} V_{nj}\langle s_m^\dagger s_j c\rangle \\ & + ig(\langle c^\dagger s_n c\rangle - \langle s_m^\dagger cc\rangle) - ig\sum_j \langle s_m^\dagger s_n s_j\rangle \\ & - i\sqrt{\kappa} f_{\rm in}(t_0-t)\langle s_m^\dagger s_n\rangle,\end{aligned} \tag{23}$$

$$\begin{aligned}\frac{d}{dt}\langle s_m^\dagger cc\rangle =& (i\Omega-\kappa)\langle s_m^\dagger cc\rangle + i\sum_{j(\neq m)} V_{jm}\langle s_j^\dagger cc\rangle - 2ig\sum_j \langle s_m^\dagger s_j c\rangle \\ & + ig\langle c^\dagger cc\rangle - 2i\sqrt{\kappa} f_{\rm in}(t_0-t)\langle s_m^\dagger c\rangle,\end{aligned} \tag{24}$$

$$\begin{aligned}\frac{d}{dt}\langle c^\dagger s_m s_n\rangle =& \left(-2i\Omega-\frac{\kappa}{2}\right)\langle c^\dagger s_m s_n\rangle - i\sum_{j(\neq m)} V_{mj}\langle c^\dagger s_j s_n\rangle \\ & - i\sum_{j(\neq n)} V_{nj}\langle c^\dagger s_m s_j\rangle - ig(\langle c^\dagger s_n c\rangle + \langle c^\dagger s_m c\rangle) \\ & + ig\sum_j \langle s_j^\dagger s_m s_n\rangle + i\sqrt{\kappa} f^*(t_0-t)\langle s_m s_n\rangle,\end{aligned} \tag{25}$$

$$\begin{aligned}\frac{d}{dt}\langle c^\dagger s_m c\rangle =& (-i\Omega-\kappa)\langle c^\dagger s_m c\rangle - i\sum_{j(\neq m)} V_{mj}\langle c^\dagger s_j c\rangle \\ & + ig\sum_j \langle s_j^\dagger s_m c\rangle - ig\sum_j \langle c^\dagger s_m s_j\rangle - ig\langle c^\dagger cc\rangle \\ & + i\sqrt{\kappa} f^*(t_0-t)\langle s_m c\rangle - i\sqrt{\kappa} f_{\rm in}(t_0-t)\langle c^\dagger s_m\rangle,\end{aligned} \tag{26}$$

$$\begin{aligned}\frac{d}{dt}\langle c^\dagger cc\rangle =& -\frac{3\kappa}{2}\langle c^\dagger cc\rangle + ig\sum_j \langle s_j^\dagger cc\rangle - 2ig\sum_j \langle c^\dagger s_j c\rangle \\ & + i\sqrt{\kappa} f^*(t_0-t)\langle cc\rangle - 2i\sqrt{\kappa} f_{\rm in}(t_0-t)\langle c^\dagger c\rangle,\end{aligned} \tag{27}$$

$$\frac{d}{dt}\langle c_3\rangle = -\frac{\kappa}{2}\langle c_3\rangle - ig\sum_j \langle s_{3,j}\rangle, \tag{28}$$

$$\begin{aligned}\frac{d}{dt}\langle s_{3,m}\rangle =& -i\Omega\langle s_{3,m}\rangle - i\sum_{j(\neq m)} V_{mj}\langle s_{3,j}\rangle - ig\langle c_3\rangle + 2ig\langle s_m^\dagger s_m c\rangle \\ & + 2i\sum_{j(\neq m)} V_{mj}\langle s_m^\dagger s_m s_j\rangle.\end{aligned} \tag{29}$$

Finally, using $\langle c_1\rangle$ and $\langle c_3\rangle$, the first- and third-order components of the output field are given, respectively, by

$$f_{\rm out}^{(1)}(r,t) = -f_{\rm in}(r-t+t_0) + i\sqrt{\kappa}\langle c_1(t-r)\rangle, \tag{30}$$

$$f_{\rm out}^{(3)}(r,t) = i\sqrt{\kappa}\langle c_3(t-r)\rangle. \tag{31}$$

It should be recalled that $\langle s_m s_n\rangle$, $\langle s_m^\dagger s_n s_l\rangle$, and $\langle c^\dagger s_m s_n\rangle$ vanish in the case of $N=1$, because $s_j s_j = 0$.

IV. THREE FORMS OF V_{ji}

The above equations are applicable to any form of the exciton hopping interaction V_{ji}. Here, we consider the following three concrete forms of V_{ji} and actually evaluate the two-photon nonlinearity β, following the formalism presented in Secs. III A and III B.

(i) *Periodic chain*. In this model, the sites are aligned one dimensionally, forming a periodic chain. Assuming that the hopping interaction exists only between nearest-neighboring sites, V_{ji} is given by

$$V_{ji} = \begin{cases} -V/2 & (|j-i| = 1 \text{ or } N-1), \\ 0 & (\text{otherwise}). \end{cases} \tag{32}$$

The one-exciton eigenstate is given by $|x_n\rangle = \sum_{j=1}^N N^{-1/2}\exp(ik_n j)s_j^\dagger|0\rangle$ where $k_n = 2\pi(n-1)/N$ $(n=1,\ldots,N)$, and its energy is given by $E_n = \Omega - V\cos k_n$. The energy diagram is shown in Fig. 2(a). It should be noted that the coupling strength between the cavity mode $(c^\dagger|0\rangle)$ and the one-exciton eigenstate $(|x_n\rangle)$ is concentrated onto the lowest eigenstate $|x_1\rangle$, whereas other eigenstates completely

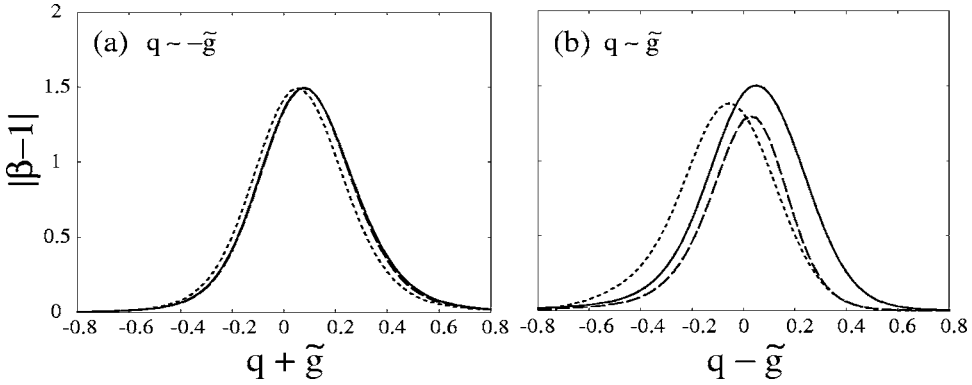

FIG. 3. Plot of $|\beta-1|$ as a function of photonic energy q. The photon energy is tuned to the lower Rabi-split frequency ($q\sim-\tilde{g}$) in (a) and to the higher one ($q\sim\tilde{g}$) in (b). Solid, dotted, and dashed lines are used to represent the results for the model (iii), (ii), and (i), respectively. The employed parameters are as follows: $N=5$, $\kappa/g=0.5$, $V/g=5$; Ω is chosen so that the lowest excitonic energy becomes zero.

lose the coupling to the cavity mode. The coupling strength between the cavity mode and the lowest state is given by $\tilde{g}=\sqrt{N}g$, suffering the size-enhancement effect.

(ii) *Nonperiodic chain*. In this model, we consider a case where the sites are aligned one dimensionally, *not* forming a periodic chain. Assuming again that the hopping interaction exists only between nearest-neighboring sites, V_{ji} is given by

$$V_{ji}=\begin{cases}-V/2 & (|j-i|=1),\\ 0 & (\text{otherwise}).\end{cases} \tag{33}$$

The one-exciton eigenstate is given by $|\mathrm{x}_n\rangle=\Sigma_{j=1}^{N}[2/N+1]^{1/2}\sin(k_n j)s_j^{\dagger}|0\rangle$ where $k_n=\pi n/(N+1)$ $(n=1,\ldots,N)$, and its energy is given by $E_n=\Omega-V\cos k_n$. The energy diagram is shown in Fig. 2(b). In this model, the coupling strength between the cavity mode ($c^{\dagger}|0\rangle$) and the one-exciton eigenstate ($|\mathrm{x}_n\rangle$) is mainly concentrated on the lowest eigenstate $|\mathrm{x}_1\rangle$, but contrarily to model (a), the coupling does not vanish for states with odd n. The coupling strength between the cavity mode and the lowest state is given by

$$\tilde{g}=g\left(\frac{2}{N+1}\right)^{1/2}\cot\left(\frac{\pi}{2(N+1)}\right)\simeq g\frac{2^{3/2}}{\pi}\sqrt{N+1}.$$

(iii) *Mean-field form*. In this model, the hopping interaction between sites is assumed to be independent of the distance between sites and is given by the following form:

$$V_{ji}=\begin{cases}-\dfrac{V}{N-1} & (j\neq i),\\ 0 & (j=i).\end{cases} \tag{34}$$

Although this form of V_{ji} seems to be rather unphysical, the equations of motion presented in Sec. III B are greatly simplified in this model, which gives a useful perspective concerning the size effects on the two-photon nonlinearity (see Sec. V). The lowest one-exciton eigenstate is given by $|\mathrm{x}_1\rangle=\Sigma_{j=1}^{N}N^{-1/2}s_j^{\dagger}|0\rangle$, whose eigenenergy is given by $E_1=\Omega-V$. The other eigenstates have $(N-1)$-fold degeneracy: the eigenenergy is given by $E_n=\Omega+V/(N-1)$ for $n=2,\ldots,N$, and the eigenstates are spanned by $N-1$ states which are orthogonal to $|\mathrm{x}_1\rangle$. The coupling strength between the cavity mode and the lowest state is given by $\tilde{g}=\sqrt{N}g$, whereas other one-exciton eigenstates lose coupling to the cavity mode.

Using these three forms of V_{ji}, we now evaluate the two-photon nonlinearity β. The system parameters are chosen as follows: $N=5$, $\kappa/g=0.5$, $V/g=5$, and Ω is chosen so that Λ (the energy of the lowest one-exciton state) becomes identical to the cavity frequency—i.e., $\Omega=V$ for models (i) and (iii) and $\Omega=V\cos[\pi/N+1]$ for model (ii). Under this choice of parameters, this cavity-exciton system is in the strong coupling regime. Then, significant nonlinearity is expected by photon pulse with $q\sim\pm\tilde{g}$ and $d\sim4/\kappa$ [10], so we fixed the photon length at $d=4/\kappa$.

In Fig. 3, $|\beta-1|$ is plotted as a function of the central frequency q of input photons. The results for $q\sim-\tilde{g}$ (lower Rabi-split frequency) and for $q\sim\tilde{g}$ (higher Rabi-split frequency) are plotted in Figs. 3(a) and 3(b), respectively. It is observed in Fig. 3(a) that the results for three models are almost coincident when the input photons are tuned to the lower Rabi frequency, whereas in Fig. 3(b) the results show quantitative difference among three models when the input photons are tuned to the higher one. This difference should be attributed to how these Rabi-split levels couple to two-exciton states, which also take part in the third-order response. Let us recall here that the central energy of excitonic states (Ω) is chosen to be positive here, so two-exciton states lie mainly in the positive-frequency region. Therefore, the lower Rabi-split state, whose energy ($-\tilde{g}$) is negative, is almost decoupled from two-exciton states, and the optical response around the lower Rabi-split level takes place almost irrespective of two-exciton states. Contrarily, the higher Rabi-split state has a positive energy and is energetically closer to two-exciton states. The optical response around this frequency region is more sensitive to the level structure of two-exciton states and, therefore, to V_{ji}.

V. *N* DEPENDENCE OF TWO-PHOTON NONLINEARITY

In the preceding section, it is observed that the two-photon nonlinearity is not sensitive to the form of V_{ji}, particularly when the input photons are tuned to the lower Rabi-split frequency. Here, we investigate the main problem of the present study: namely, the system-size dependence of the two-photon nonlinearity. To this end, we are based on model (iii), where V_{ji} is given by the mean-field form. In this case, the equations of motion are greatly simplified; the expectation values appearing in these equations become independent of the site index. Thus, we use the following notations, such

as $N^{1/2}\langle s_m\rangle \equiv \langle S\rangle$, $N\langle s_m^\dagger s_n\rangle \equiv \langle S^\dagger S\rangle$, and $N^{3/2}\langle s_m^\dagger s_n s_l\rangle \equiv \langle S^\dagger SS\rangle$. Furthermore, using $\tilde{g}$ $(=\sqrt{N}g)$ and Λ $(=\Omega - V$, the energy of the lowest excitonic state) the equations of motion for the first-order quantities are rewritten as

$$\frac{d}{dt}\langle c_1\rangle = -\frac{\kappa}{2}\langle c_1\rangle - i\tilde{g}\langle S_1\rangle - i\sqrt{\kappa}f(t_0 - t), \tag{35}$$

$$\frac{d}{dt}\langle S_1\rangle = -i\Lambda\langle S_1\rangle - i\tilde{g}\langle c_1\rangle, \tag{36}$$

and the equations of motion for the second-order quantities are given by

$$\frac{d}{dt}\langle S^\dagger S\rangle = -i\tilde{g}(\langle S^\dagger c\rangle - \text{c.c.}), \tag{37}$$

$$\frac{d}{dt}\langle S^\dagger c\rangle = \left(i\Lambda - \frac{\kappa}{2}\right)\langle S^\dagger c\rangle - i\tilde{g}\langle S^\dagger S\rangle + i\tilde{g}\langle c^\dagger c\rangle - i\sqrt{\kappa}f(t_0 - t) \times \langle S_1\rangle^*, \tag{38}$$

$$\frac{d}{dt}\langle c^\dagger c\rangle = -\kappa\langle c^\dagger c\rangle + i\tilde{g}(\langle S^\dagger c\rangle - \text{c.c.}) + (i\sqrt{\kappa}f^*(t_0 - t)\langle c_1\rangle + \text{c.c.}), \tag{39}$$

$$\frac{d}{dt}\langle SS\rangle = -2i\left(\Lambda + \frac{V}{N-1}\right)\langle SS\rangle - 2i\tilde{g}\langle Sc\rangle, \tag{40}$$

$$\frac{d}{dt}\langle Sc\rangle = \left(-i\Lambda - \frac{\kappa}{2}\right)\langle Sc\rangle - i\tilde{g}\langle cc\rangle - i\frac{N-1}{N}\tilde{g}\langle SS\rangle - i\sqrt{\kappa}f(t_0 - t)\langle S_1\rangle, \tag{41}$$

$$\frac{d}{dt}\langle cc\rangle = -\kappa\langle cc\rangle - 2i\tilde{g}\langle Sc\rangle - 2i\sqrt{\kappa}f(t_0 - t)\langle c_1\rangle, \tag{42}$$

and the equations of motion for the third-order quantities are given by

$$\frac{d}{dt}\langle S^\dagger SS\rangle = -i\left(\Lambda + \frac{2V}{N-1}\right)\langle S^\dagger SS\rangle + i\tilde{g}(\langle c^\dagger SS\rangle - 2\langle S^\dagger Sc\rangle), \tag{43}$$

$$\frac{d}{dt}\langle S^\dagger Sc\rangle = -\frac{\kappa}{2}\langle S^\dagger Sc\rangle + i\tilde{g}(\langle c^\dagger Sc\rangle - \langle S^\dagger cc\rangle) - i\tilde{g}\frac{N-1}{N}\langle S^\dagger SS\rangle - i\sqrt{\kappa}f(t_0 - t)\langle S^\dagger S\rangle, \tag{44}$$

$$\frac{d}{dt}\langle S^\dagger cc\rangle = (i\Lambda - \kappa)\langle S^\dagger cc\rangle + i\tilde{g}\langle c^\dagger cc\rangle - 2i\tilde{g}\langle S^\dagger Sc\rangle - 2i\sqrt{\kappa}f(t_0 - t)\langle S^\dagger c\rangle, \tag{45}$$

$$\frac{d}{dt}\langle c^\dagger SS\rangle = \left\{-2i\left(\Lambda + \frac{V}{N-1}\right) - \frac{\kappa}{2}\right\}\langle c^\dagger SS\rangle - 2i\tilde{g}\langle c^\dagger Sc\rangle + i\tilde{g}\langle S^\dagger SS\rangle + i\sqrt{\kappa}f^*(t_0 - t)\langle SS\rangle, \tag{46}$$

$$\frac{d}{dt}\langle c^\dagger Sc\rangle = (-i\Lambda - \kappa)\langle c^\dagger Sc\rangle + i\tilde{g}\langle S^\dagger Sc\rangle - i\tilde{g}\langle c^\dagger cc\rangle - i\tilde{g}\frac{N-1}{N}\langle c^\dagger SS\rangle + i\sqrt{\kappa}f^*(t_0 - t)\langle Sc\rangle - i\sqrt{\kappa}f(t_0 - t) \times \langle c^\dagger S\rangle, \tag{47}$$

$$\frac{d}{dt}\langle c^\dagger cc\rangle = -\frac{3\kappa}{2}\langle c^\dagger cc\rangle + i\tilde{g}\langle S^\dagger cc\rangle - 2i\tilde{g}\langle c^\dagger Sc\rangle + i\sqrt{\kappa}f^*(t_0 - t) \times \langle cc\rangle - 2i\sqrt{\kappa}f(t_0 - t)\langle c^\dagger c\rangle, \tag{48}$$

$$\frac{d}{dt}\langle c_3\rangle = -\frac{\kappa}{2}\langle c_3\rangle - i\tilde{g}\langle S_3\rangle, \tag{49}$$

$$\frac{d}{dt}\langle S_3\rangle = -i\Lambda\langle S_3\rangle - i\tilde{g}\langle c_3\rangle + \frac{2i\tilde{g}}{N}\langle S^\dagger Sc\rangle - \frac{2iV}{N}\langle S^\dagger SS\rangle. \tag{50}$$

It should be recalled again that, for $N=1$, $\langle SS\rangle = \langle S^\dagger SS\rangle = \langle c^\dagger SS\rangle = 0$ due to the Pauli exclusion principle. These equations are further simplified in the following two limiting cases.

A. Quantum-dot limit

Because $2V$ represents the bandwidth of one-exciton states (see Fig. 2) and there are N levels in this band, $2V/(N-1)$ represents the mean energy separation between one-exciton levels. First, we consider a situation where the mean energy separation is much larger than other relevant energies; i.e., $2V/(N-1) \gg \Lambda$, $\tilde{g}$, κ is satisfied. Such a situation is widely observed in quantum-dot systems. In this situation, the excitonic states other than the lowest one are highly off resonant to the cavity mode. It is therefore expected that these excitonic states play almost no role in the optical response and that an effective two-level system (composed by the ground and the lowest exciton state) is realized in this limit.

By taking the limit of $2V/(N-1) \to \infty$, we can analytically confirm the validity of this expectation. Namely, the equations of motion, Eqs. (35)–(50), are reduced to those for a single two-level $(N=1)$ case, with the transition energy Λ and the size-enhanced cavity-exciton coupling $\tilde{g}$ $(=\sqrt{N}g)$. In the limit of $2V/(N-1) \to \infty$, applying the adiabatic approximation to Eqs. (40), (43), and (46), $\langle SS\rangle$, $\langle S^\dagger SS\rangle$, and $\langle c^\dagger SS\rangle$ are given by

$$\langle SS\rangle \simeq -\tilde{g}\frac{N-1}{V}\langle Sc\rangle, \tag{51}$$

$$\langle S^\dagger SS\rangle \simeq \tilde{g}\frac{N-1}{2V}(\langle c^\dagger SS\rangle - 2\langle S^\dagger Sc\rangle), \tag{52}$$

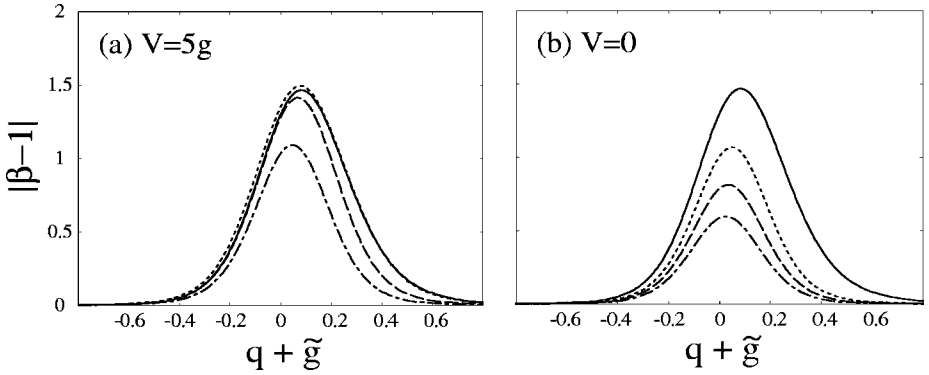

FIG. 4. Plot of $|\beta-1|$ as a function of q, around the lower Rabi-split frequency. The coherent length of photons is chosen at $d=4/\kappa$. The site number N is 1 (solid line), 5 (dotted line), 10 (dashed line), and 20 (dot-dashed line). The system parameters are chosen as follows: $\kappa/g=0.5$, $\Omega=V$ (which results in $\Lambda=0$), and $V/g=5$ in (a) and $V/g=0$ in (b).

$$\langle c^\dagger SS\rangle \simeq \frac{N-1}{2V}[-2i\tilde{g}\langle c^\dagger Sc\rangle + i\tilde{g}\langle S^\dagger SS\rangle + i\sqrt{\kappa}f^*(t_0-t)\langle SS\rangle], \tag{53}$$

all of which vanishes as $2V/(N-1)\to\infty$:

$$\langle SS\rangle, \langle S^\dagger SS\rangle, \langle c^\dagger SS\rangle \to 0. \tag{54}$$

Using Eq. (52), the driving terms for $\langle c_3\rangle$ and $\langle S_3\rangle$—i.e., the third and fourth terms in the on the right-hand side of Eq. (50)—are reduced to the following form:

$$\frac{2i\tilde{g}}{N}\langle S^\dagger Sc\rangle - \frac{2iV}{N}\langle S^\dagger SS\rangle \simeq 2i\tilde{g}\langle S^\dagger Sc\rangle - i\frac{N-1}{N}\tilde{g}\langle c^\dagger SS\rangle \to 2i\tilde{g}\langle S^\dagger Sc\rangle. \tag{55}$$

Substituting the limiting values (54) and (55) into Eqs. (35)–(50), we can confirm that the resultant equations of motion coincides with those for the case of a single two-level system ($N=1$), with the transition frequency Λ and the size-enhanced coupling $\tilde{g}$. Therefore, the excitonic system can be regarded as a quantum dot, when V is large and N is small enough to satisfy $2V/(N-1)\gg\Lambda$, $\tilde{g}$, κ. However, as N gets larger, the picture of quantum dot becomes less valid and the two-photon nonlinearity gets weaker, as will be discussed in the next subsection.

B. Bulk limit

Next, we consider the bulk limit $N\to\infty$. In this limit, where $V/(N-1)\to 0$ and $(N-1)/N\to 1$, it is easily confirmed that V and N dependences are lost in Eqs. (35)–(48), except for the renormalization of the coupling constant $\tilde{g}$ $(=\sqrt{N}g)$. This fact indicates that the expectation values appearing in Eqs. (35)–(48) become essentially independent of the hopping V and the system size N if input photons are adequately tuned to the Rabi-split frequency $\pm\tilde{g}$. Turning our attention to Eqs. (49) and (50), the driving terms for $\langle c_3\rangle$ and $\langle S_3\rangle$ scale as $(2i\tilde{g}/N)\langle S^\dagger Sc\rangle \sim N^{-1/2}$ and $(2iV/N)\langle S^\dagger SS\rangle \sim N^{-1}$. Therefore, the third-order output field $f_{out}^{(3)}$, which is proportional to $\langle c_3\rangle$ [see Eq. (31)], would scale as $f_{out}^{(3)}\sim N^{-1/2}$. Remembering that $\beta-1$ is proportional to $f_{out}^{(3)}$ [see Eq. (8)], it is therefore expected that the magnitude of the two-photon nonlinearity $|\beta-1|$ would scale as $|\beta-1|\sim N^{-1/2}$.

C. Crossover between two limits

In this subsection, we visualize the size effect on the two-photon nonlinearity with numerical examples and observe the crossover between the dot limit and the bulk limit. In Fig. 4, $|\beta-1|$ is plotted as a function of the photon frequency q. Under the choice of parameters in Fig. 4(a), the condition of the dotlike behavior ($[2V/(N-1)\gtrsim\Lambda,\tilde{g},\kappa]$ is satisfied when $N\lesssim 5$. Numerical results in Fig. 4(a) show that the result for a genuine two-level system ($N=1$) is almost reproduced for $N\lesssim 10$, in agreement with our expectation. Contrarily, under the choice of parameters in Fig. 4(b), the dotlike behavior is not expected for any $N(\neq 1)$. We can confirm this expectation in Fig. 4(b), where $|\beta-1|$ decreases monotonously as N is increased.

In Fig. 5, β is plotted on the complex plane varying the system size N, where the almost optimum pulse shape for inducing nonlinear effects ($d=4/\kappa, q=-\tilde{g}$) is employed for each N. In Fig. 5(a), where $V\neq 0$, β is kept almost unchanged for $N\lesssim 10$, indicating that the system is in the quantum-dot region. Contrarily, in Fig. 5(b), where $V=0$ and there is no quantum-dot region, the two-photon nonlinearity gets weaker monotonously as N is increased. It is commonly observed in both figures that the two-photon nonlinearity gets weaker as the system size N becomes larger ($\beta\to 1$ as $N\to\infty$), as expected. For large N, the nonlinear effect mainly appears in the phase of β, keeping $|\beta|\simeq 1$. In other words, for large N, the nonlinear effect appears as the nonlinear phase shift in the output wave function, whereas the shape of the output pulse is almost unchanged from the linear case.

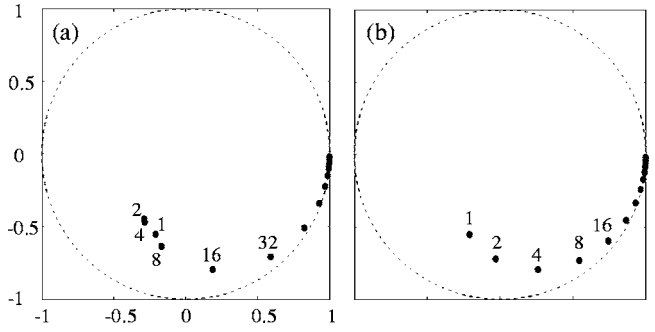

FIG. 5. Plot of β on the complex plane. The dotted line shows the unit circle. The integers near each point represent the system size N. For each N, the almost optimum pulse shape ($d=4/\kappa$, $q=-\tilde{g}$) is employed. The system parameters are the same as Fig. 4.

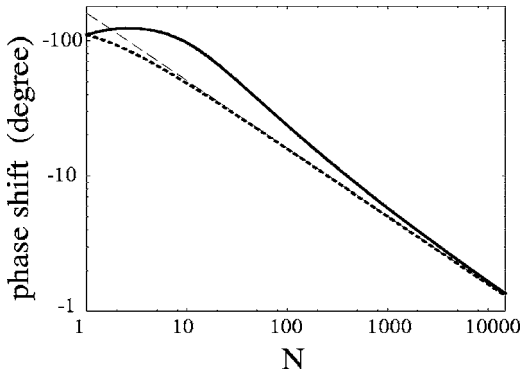

FIG. 6. Plot of the nonlinear phase shift θ as a function of the system size N. The solid and dashed lines represent the results for $V/g=5$ and 0, respectively. (Other parameters are the same as Fig. 5.) The thin dotted line is drawn by $\theta=160^{\circ}\times N^{-1/2}$, by which numerical results are well fitted for large N.

In Fig. 6, the nonlinear phase shift is plotted as a function of the system size N, where a solid (dotted) line is used to represent the numerical results for the $V\neq 0$ ($V=0$) case. When the system size N is small, the $V\neq 0$ system gives a larger phase shift than the $V=0$ system. However, as N gets larger, the discrepancy between the two gradually disappears. It can be confirmed that, as $N\rightarrow\infty$, the numerical results follow the $N^{-1/2}$ rule ($\theta=160^{\circ}\times N^{-1/2}$, thin dashed line), as predicted.

Combining the quantum-dot and bulk limits, the N dependence of the two-photon nonlinearity is summarized as follows: When V is large and N is small enough to satisfy $2V/(N-1)\gtrsim\Lambda$, $\tilde{g}$, κ, the excitonic system can be considered as a single quantum dot, which behaves as a single two-level entity with an size-enhanced coupling $\tilde{g}$. As N gets larger, the magnitude $|\beta-1|$ of the two-photon nonlinearity is decreased (Fig. 4) and the nonlinearity tends to appear as the phase of β: namely, the nonlinear phase shift (Fig. 5). Finally, in the bulk limit ($N\rightarrow\infty$), the system becomes independent of V and the nonlinear phase shift follows the $N^{-1/2}$ rule.

VI. SUMMARY

In summary, we have investigated the two-photon nonlinearity obtained by a Frenkel excitonic system placed inside of a cavity, aiming at clarifying how the nonlinear effects depends on the system size N. The model is applicable to many kinds of actual nonlinear optical agents, such as molecular aggregates and semiconducting particles. In Sec. II, the theoretical model and the measure β of nonlinearity is presented, and in Sec. III the method for evaluation of β is described. In Sec. IV, we have numerically evaluated β using three concrete forms of V_{ji} (exciton hopping interaction); it was revealed there that three models give qualitatively similar results, particularly when the input photons are tuned to the lower Rabi-split frequency. In Sec. V based on the mean-field form of V_{ji}, we have investigated the size dependence of β both analytically and numerically. If N is small and the mean energy separation $[V/(N-1)]$ is larger than other relevant energies, the excitonic system can be regarded as a single two-level system with the size-enhanced coupling constant $\tilde{g}$ to the cavity mode and a large nonlinear effect results. As the system size N gets larger, the nonlinear effect gets smaller. In the bulk limit ($N\rightarrow\infty$), the nonlinear phase shift scales as $N^{-1/2}$.

The above conclusions are drawn within the model of noninteracting Frenkel excitons, where the origin of nonlinearity is solely attributed to saturation effect in each site. However, it should be remarked that, in semiconducting materials, for example, the excitonic interaction serves as another important source of optical nonlinearity, which is expected to increase nonlinear effects in general. A more rigorous investigation taking account of this point is left as a future problem.

ACKNOWLEDGMENTS

The authors are grateful to M. Bamba, H. Ajiki, and K. Edamatsu for fruitful discussions. This research is partially supported by Japan Society of Promotion of Science, Grant-in-Aid for Scientific Research (A), No. 16204018, 2004.

[1] Y. R. Shen, *The Principles of Nonlinear Optics* (Wiley, New York, 1984).
[2] Q. A. Turchette, R. J. Thompson, and H. J. Kimble, Appl. Phys. B: Lasers Opt. **60**, S1 (1995).
[3] Q. A. Turchette, C. J. Hood, W. Lange, H. Mabuchi, and H. J. Kimble, Phys. Rev. Lett. **75** 4710 (1995).
[4] S. Takeuchi, Opt. Lett. **26**, 843 (2001).
[5] K. Edamatsu, R. Shimizu, and T. Itoh, Phys. Rev. Lett. **89**, 213601 (2002).
[6] K. Edamatsu, G. Oohata, R. Shimizu, and T. Itoh, Nature (London) **431**, 167 (2004).
[7] G. J. Milburn, Phys. Rev. Lett. **62** 2124 (1989).
[8] M. A. Nielsen and I. L. Chuang, *Quantum Computation and Quantum Information* (Cambridge University Press, Cambridge, England, 2000).
[9] H. F. Hofmann, K. Kojima, S. Takeuchi, and K. Sasaki, Phys. Rev. A **68**, 043813 (2003).
[10] K. Koshino and H. Ishihara, Phys. Rev. A **70**, 013806 (2004).
[11] E. Hanamura, Phys. Rev. B **37**, 1273 (1988).
[12] K. Koshino and H. Ishihara, Phys. Rev. Lett. **93**, 173601 (2004).
[13] *Cavity Quantum Electrodynamics*, edited by P. R. Berman (Academic, San Diego, 1994).
[14] H. F. Hofmann and G. Mahler, Quantum Semiclassic. Opt. **7**, 489 (1995).
[15] D. F. Walls and G. J. Milburn, *Quantum Optics* (Springer, Berlin, 1995).